Optical transmittance based store and forward routing in satellite networks

András Mihály, and László Bacsárdi, *Member, IEEE*

Abstract—Quantum computing will play a crucial part in our security infrastructure for the coming years. Quantum networks can consist of direct optical fiber or free-space links. With the use of satellite channels, we can create a quantum network with higher coverage than using optical fibers where the distances are limited due to the properties of the fiber. One of the highest drivers of cost for satellite networks, apart from the cost of the technology needed for such systems, are the costs of launching and maintaining said satellites. By minimizing the satellites needed for a well-functioning quantum network, we can decrease said network's cost, thus enabling a cheaper quantum internet. In this paper, we present an optical transmittance-based routing algorithm with which it is possible to conduct successful quantum entanglement transfer between terrestrial nodes.

Index Terms—quantum satellite, quantum satellite network, routing in scarce satellite networks, quantum entanglement

I. INTRODUCTION

PUBLIC-key cryptography is a part of our everyday life. It is used as a key security component in banks, websites, and almost everything where there is a need to provide secure communication to multiple clients. With the impending arrival of quantum computers, with which (thanks to algorithms like Shor's [1]) we will be able to crack most of the public-key encryptions used today, there is an ever-growing risk to these systems.

By utilizing quantum computing, we can not only break one of today's most used encryptions (RSA) but also speed up the calculation of various problems. Using Groover's algorithm, we can find a record in unordered data in $\sqrt{N}$ time [2], or even extreme values [3]. With the help of quantum computing, we can solve problems like multi-user detection [3] or optimal resource distribution [4]. Quantum key distribution (QKD) is a part of quantum communication with which we can create theoretically unbreakable networks. These key distribution protocols suppose that the other party can and will use every tool that our current understanding of physics does not forbid. Hence it can provide lasting future proof of security.

Quantum networks although, provide one of the most secure environments for communication, their physics-enabled security has its drawbacks against classical networks. The greatest one is what provides most of its security, is the no-cloning

The authors are with the Department of Networked Systems and Services, Budapest University of Technology and Economics, Budapest, Hungary. (e-mail: andras.mihaly.1998@gmail.com, bacsardi@hit.bme.hu)

theorem [5]. This theorem states that we cannot measure the complete state of a quantum bit without destroying it, thus we cannot make deep copies of it. This prevents us from creating routers or signal enhancers like in classical networks or broadcast quantum information. This, however, doesn't mean that we cannot create quantum communication networks. For example, by using the side effect of the bell state measurement [6], we can swap the entanglement of quantum bits [7]. This is the basis for the quantum repeaters referred to in this paper, which are detailed in the Section III-C.

Although the aforementioned quantum systems are still years away, one could, for example, save the encrypted traffic going through a busy node for him to decrypt it later. The validity of this attack vector can be easily noticed as internet users transmit information that can be valuable even in years [8]. For example, if somebody would collect the Social Security Number (SSN) of millions of American residents, it could be devastating even if the information would only be available in 20 years.

In light of these facts, there are multiple projects all over the world, from China to Europe [9–12], to build secure quantum communication networks. These early plans primarily rely on free-space quantum communication channels, which provide better coverage at a lesser infrastructure cost. We can further increase our transmission rate by using low earth orbit (LEO) satellites.

Satellite-based networks have better coverage and in some cases, a better noise rate to the channel length. Not considering the cost of technology development which is needed for a high-reliability satellite-based quantum system, one of the highest drivers of cost for these networks is the cost of launching and maintaining satellites.

With the evolution of quantum memories[13], quantum systems do not require a consistent stream of quantum bits to function. As such we could create a satellite-based quantum network that transfers the quantum data at a reasonable rate but not continuously. With this, we could enable a quantum network with as little as 32 quantum satellites instead of the hundreds needed for continuous communication [14]. In our work, we created an algorithm that maximizes the transfer rate of entangled quantum bits over scarce satellite networks. This was achieved by making every node keep its "cargo" until the best possible next node becomes available.

The structure of the paper is as follows: in Section II we detail our data structure and the setup of the simulation. In Section III, we present our algorithm for generating routes in scarce satellite networks. Section IV concludes our paper.

II. RELATED WORKS

Satellite-based quantum networks and optimal architectures for such systems are a hot topic even in recent years. It comes as no surprise since such a network could provide global coverage. Most quantum satellite architectures fall into two categories. The first architecture exists only for creating keys between the end-nodes. This is done by generating keys between the intermediary nodes. With the use of those keys, it is possible to create a key between the end nodes. The benefits of using this architecture are a cheaper cost and simple implementation. On the other hand, this type of system can only be used for QKD and requires the users to trust each node. The second type of satellite communication architecture uses a technique called nested purification or purify-and-swap[15]. With the help of nested purification, it is possible to create entangled quantum bits in distant nodes. By using the entangled quantum bits, the end nodes can use quantum teleportation to exchange quantum bits between each other. This architecture can be used not only for QKD but for communication between quantum computers. This architecture is complex and limited by the evolution of more quantum components such as the quantum memory and the quantum entanglement generator.

One of the few recent publications that use a QKD-only architecture is the one published by the University of California and Beijing University of Posts and Telecommunications[16]. In a joint paper, the two universities proposed a two-layer satellite network. The lower layer is composed of 66 LEO satellites and the upper layer is composed of 3 geosynchronous earth orbit (GEO) satellites. In their research, they also proposed an algorithm for calculating optimal routes. As hinted before, this architecture uses a trusted node-based architecture. Using this kind of architecture means the hardware needed for the satellites is less complex. On the other hand, compromising a single intermediary node can lead to the compromise of the whole system.

As we mentioned in the first paragraph of this chapter, most research today uses an entanglement-based architecture. A highly influential research paper using this architecture was released in December 2019. "Spooky action at a global distance: analysis of space-based entanglement distribution for the quantum internet" [14] was a joint work by multiple universities around the globe. The article proposed an algorithm for determining optimal satellite configurations while maintaining continuous coverage. Their simulation consisted of 200 satellites and could achieve an average entangled quantum bit transfer of 1321/sec, which is 4755600 entangled quantum bits every hour. Due to the properties of the purify and swap architecture, the resulting satellite system's security cannot be compromised by a rouge or hacked intermediary node.

By looking at the current state of quantum satellite networks, it is clear that we will reach a working product in the near future, but it is also evident that most constellations work with a high satellite count and almost continuous coverage. These properties of the network result in an increase in its cost. In our research, we tried to minimalize the price of a network by suggesting a network composition that would require significantly fewer satellites. But with the low satellite count, our satellite architecture needs a new type of routing to function. This algorithm is detailed later in our paper.

III. OUR SETUP

Our setup consists of two main modules: an orbital propagation and a routing module. The orbital propagation module is responsible for the simulation of satellite orbits. In addition, the routing module's main task is finding an optimal route through the satellite network.

A. Time-dependent graphs

Time-dependent graphs [17] can be related to many names, including temporal graphs, evolving graphs, time-varying graphs, historical graphs, and many more. In our research, we will use the term time-varying graphs. Time-varying graphs are perfect for modeling data networks, which change over time. We used the approach in which the weights on the edges are the time instances they are available. Meaning the edge $\xrightarrow{<t_1,t_2>}$ between nodes n_1 and n_2 shows that the node n_1 will have a valid edge to node n_2 in the time instances t_1 and t_2. Instead of time instances, it is also possible to time arrays to define a larger timeframe.

B. Data representation

In our research, we needed a structure to model the changing network of satellites. For this purpose, we have chosen the time-varying graph (TVG). Time-varying graphs are special types of graphs that change over time in a predetermined manner. In our model, the graph nodes represent the satellite and terrestrial nodes in the network. As it is illustrated in Figure 1, between nodes n_1 and n_2 we draw an edge $\xrightarrow{[t_1,t_2]\ \mu[...]}$, if there is a time interval $[t_1, t_2]$ where n_1 and n_2 are visible to each other and in that interval, the optical transmittance is $\mu_1, \mu_2, ..., \mu_{t_2-t_1}$.
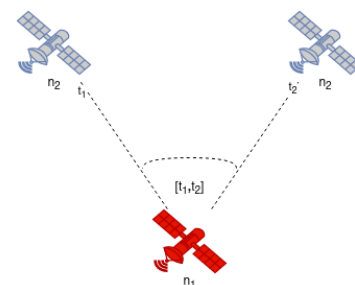

Fig. 1. Visualization of the data representation. The satellites n_1 and n_2 are represented as nodes. The changes in the visibility between them are modeled as the edge between these nodes.

C. Theoretical architecture of the quantum satellite nodes

In our work, we used an abstracted view of quantum satellites. These satellites, as detailed in Figure 2, consist of three main modules:

1) **Quantum CPU:** the quantum processor's main job is to perform the bell state measurement on the two quantum memories, swapping their entanglement [18].
2) **Quantum memory:** the quantum memory is being used to store the entangled quantum bits received from the previous node and the current node.
3) **Entangled quantum bit generator:** the entangled bit generator is responsible for providing the entangled quantum bits for the current and the next node.
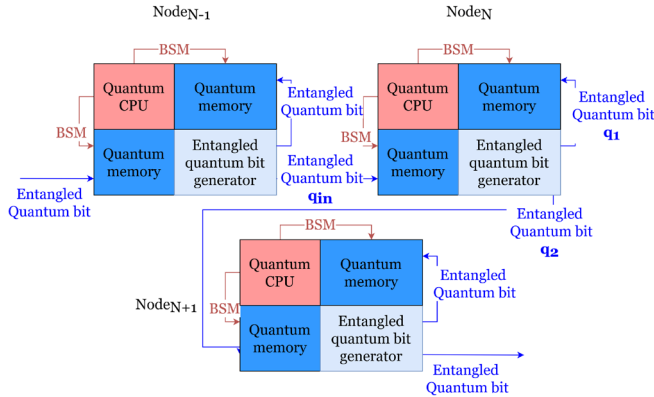

Fig. 2. Abstract model of the quantum satellite architecture consisting of three nodes.

The system works as follows: First, the entangled quantum bit generator provides an entangled pair of quantum bits q_1 and q_2 for the current Node_N and the next Node_{N+1}. These quantum bits then are stored in the quantum memories of the nodes. Node_N can transfer the q_{in} input quantum entanglement to Node_{N+1} by swapping the entanglement between quantum q_{in} and q_1. After the procedure, the quantum bit at the Node_{N+1} will be entangled with the quantum bit located in the quantum memory of Node_{N-1}.

D. Orbital propagation module

The orbital propagation module has multiple satellite orbit-related tasks. These are in the order of usage:
1) Loading the Keplerian orbital data for the satellite orbits.
2) Calculate the changes in the satellite system provided, using the orekit space dynamics library [19].
3) Generating the visibility intervals between each node.
4) Calculating the optical transmittance for each visibility interval.
5) From the optical transmittance values and visibility intervals create the time-varying graph of the system.

E. Routing module

The routing module uses the time-varying graph generated by the orbital propagation module. By using the algorithms described in Section IV, this module calculates an optimal sequence of nodes to transmit our quantum data through. The specialty of our algorithm is that it does not require the created path to be continuous between the two end nodes. It can be thought of as a postal service sending packets of quantum data

(eg., quantum entanglements) between nodes, resting the data at one node until the next optimal one becomes available.

IV. OPTICAL TRANSMITTANCE BASED STORE AND FORWARD ROUTING ALGORITHM

As mentioned before, our research and thus our algorithm focuses on finding the best route in sparsely populated satellite networks. We modeled the network with the use of time-varying graphs, where edges represent visibility between nodes. The edges contain the timeframes of the visibility and the optical transmittance for each timeframe. The optical transmittance was calculated with the help of QSCS [20]. The result is an extended time-varying graph (ETVG).

Our algorithm can be divided into main 4 parts:
- **Main loop**
- **FindBestRoute**
- **isViableEdge**
- **Optimize**

A. Main loop

The main loop is the starting point of our algorithm, it calls the *FindBestRoute* algorithm for each input's node each edge.

Algorithm 1 Main loop

   Input: ETVG, $N[...]$ list of nodes to generate paths between

   Output: Optimal paths

for each n node in N **do**
   for index i of edges in n **do**
      $FindBestRoute(ETVG, n, i)$
   end for
end for

B. FindBestRoute

This sub-algorithm calculates the best path for each edge of the starting node.

Algorithm 2 FindBestRoute

   Input: ETVG, node n and index i
   Output: Optimal paths

$paths \leftarrow i$-th edge of the start node
$out \leftarrow \{\}$
$tmp \leftarrow \{\}$
while paths can be increased **do**
   for $path$ in paths **do**
      for $edge$ in $path$ **do**
         if $isViableEdge(edge, path)$ **then**
            $opt \leftarrow Optimize(edge, path)$
            if $edge$ point to destination **then**
               $out \leftarrow opt$
            else if then
               $tmp \leftarrow opt$
            end if
         end if
      end for
   end for
end while

C. isViableEdge

The algorithm checks if the edge with the given path meets the criteria for a valid path. The path needs to meet the following criteria for the edge to be counted as a valid extension:

- The time distance between the paths first edges end and last edges start should be less than the maximum allowed.
- The edge should lead to a node the path doesn't already contain.
- The new edges end has to be later than the previous paths last edges start time

---

Algorithm 3 isViableEdge

    Input: Edge, Path
    Output: True/False
$\delta \leftarrow$ edge.startTime $-$ firstEdgeOfPath.endTime
if $\delta \geq$ global maximum path duration **then**
    return False
end if
if Path doesn't contain the node the edge is leading to **then**
    return edge.endTime $>$ lastEdgeOfPath.startTime
end if
return False

D. Optimize

This sub-algorithm uses a subset of the 13 base relations between two intervals proposed by Allen [21]. Optimization is needed in two cases. The first when the second edge finishes faster than the first one. This would mean that we are still sending data to a node that stopped transmitting forward, hence the need to cut down the said part. The second is when the second edge starts earlier than the first one. In that case, we need to cut down that part, since we cannot forward transmission that hasn't even been sent.

Algorithm 4 Optimize

    Input: Edge, Path
    Output: Optimized path
$path \leftarrow Path + Edge$
for each e_1 e_2 adjacent edge pairs in the path **do**
    $t_1 \leftarrow e1.startTime$
    $t_2 \leftarrow e1.endTime$
    $t_3 \leftarrow e2.startTime$
    $t_4 \leftarrow e2.endTime$
    if $t_4 < t_2$ **then**
        cut the end of e_1 by $t_2 - t_4$
    end if
    if $t_3 < t_1$ **then**
        cut the start of e_2 by $t_1 - t_3$
    end if
end for

V. RESULTS

In our research, we compared our algorithm across multiple types of satellite constellations. We used two main architecture types, cross, and retrograde, along four-four constellations. We simulated multiple ground stations covering the whole globe to get a more in-depth understanding of our algorithm. We have chosen a starting ground station, for each architecture and calculated the optical throughput for every other ground station.

By multiplying the optical transmittance for each timeframe with the current best realized photonic entangled quantum bit generators output [22] we calculated the throughput for every edge. The overall throughput of a path was determined by finding its smallest edges throughput. In our simulations, we used the following default values:

- **Default satellite orbit:** $a : 1000[km]$, $e : 0.0002090$, $i : 56.0568°$, $\Omega : 0°$, $\omega : 0°$, $\theta : 18.0$
- **Max path duration:** 3600 [s]
- **Efficiency of the entangled quantum bit generator:** 3.5 [kHz]
- **Simulation Time:** 14400 [s].
- **Test ground station's locations:** Lattitude: one for every 10°, Longitude: one for every: 15°
- **Starting ground station location:** Lattitude: 0°, Longitude: 0°

A. Input Orbits

In our research, we modeled two types of satellite architectures along with four satellite systems with a varying number of satellites. The first one, we called Retrograde architecture since every second satellite's inclination was rotated by 180°. The second architecture we used was the Cross architecture, here every second satellite's inclination was rotated by 90°.

The four satellite systems we used were composed of a default Keplerian orbit rotated along the longitude of the ascending node (Ω) and argument of periapsis (ω) in increments of 45°. The differences between the four systems are the intervals of these rotations, as detailed in Table I.

TABLE I
THE SATELLITES SYSTEMS USED IN THE SIMULATIONS. THE TABLE CONTAINS THE FOLLOWING FOR EACH SYSTEM: NAME, NUMBER OF SATELLITES, THE LONGITUDE OF THE ASCENDING NODE (Ω), AND ARGUMENT OF PERIAPSIS (ω).

Name	Number of satellites	Ω interval	ω interval
Low	12	$0 - 180°$	$0 - 180°$
LOWMid$_1$	32	$0 - 180°$	$0 - 360°$
LOWMid$_2$	32	$0 - 360°$	$0 - 180°$
MID	64	$0 - 360°$	$0 - 360°$

B. Retrograde architecture

The retrograde satellite architecture uses the default satellite orbit, which had its inclination shifted by 180° for every second satellite. By rotating the inclination of the satellite by 180°, we get an almost frontal collision track for our satellites. Consequently, the resulting satellite visibility intervals will be the shortest that is possible at these speeds. In other

Optical transmittance based store and forward
routing in satellite networks

words, retrograde architecture works with visibility intervals that are shorter in time but have a higher occurrence ratio. The average throughput of the systems can be seen in Figure 3. The averages here indicate the cumulation of the whole systems throughput between every terrestrial node (in this case, cities). As it can also be seen in the mentioned Figure, despite both consisting of 32 satellites, systems LOWMID1 and LOWMID2 have a different rate of average entangled quantum bits per hour (AEQ/h). As these systems differ only in the intervals of the used Ω and ω values, so we can conclude that the values used for said intervals can affect the systems AEQ/h. Apart from said differences, we can see that using the retrograde architecture, with only 32 satellites we can create a system that has an average AEQ/h of 9800. In the case of the bigger (MID) system, it could reach an average AEQ/h of almos 20000.
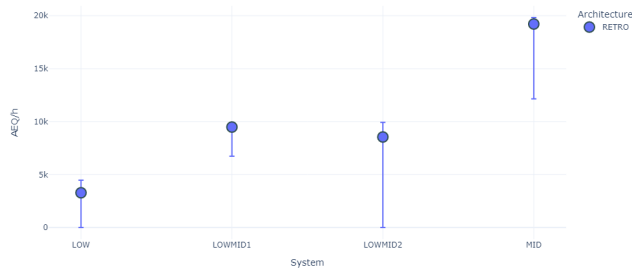

Fig. 3. Error bar plots showing the average, minimum, and maximum AEQ/h generated between the starting ground station and the test nodes for each retrograde architecture-based system. The average is noted with the blue marker, while the minimum and maximum values are indicated with the error bars.

C. Cross architecture

The cross satellite orbit architecture, like the retrograde, uses the default satellite orbit. Unlike retrograde architecture, cross-architecture shifts its orbits inclination only by 90°. By shifting by a significantly smaller value, the resulting network will produce visibility intervals that are longer in time but rarer in occurrence.
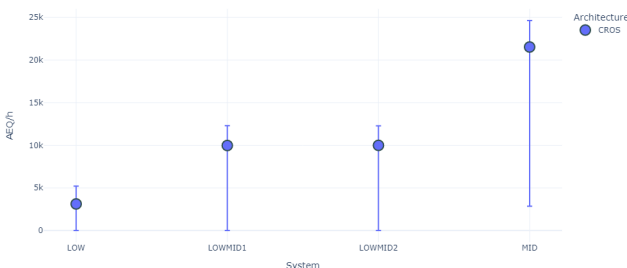

Fig. 4. Error bar plots showing the average, minimum, and maximum AEQ/h generated between the starting ground station and the test nodes for each cross architecture-based system. The average is noted with the blue marker, while the minimum and maximum values are indicated with the error bars.

As we can see in Figure 4, the resulting averages and intervals of the simulated network are significantly different. Neither LOWMID1 nor LOWMID2 satellite systems provide a full coverage, as both of their minimal AEQ/h value is 0. As it can also be seen in Figure 4, using 64 satellites we can reach an average AEQ/h of 21000, with a maximum value of more than double.

VI. CONCLUSION

In our research, we created 4-4 systems using two architectures. The architectures only differed in the angle of intersection between satellites. These angles were 180° in the case of the retrograde architecture and 90° in the case of the cross-architecture. All satellites systems used were only different in the intervals used for Ω and ω. Creating the systems in such a way, we could locate the variables responsible for changes in the throughput of the system. Looking at Figure 5, we can observe the differences between the two architectures. The first difference is one that was touched on in the previous chapter. By only changing the architecture used in systems LOWMID1 and LOWMID2, they performed differently in comparison to each other. In the case of cross-architecture, the both systems performed at the almost the same level but in the case of retrograde architecture, the LOWMID2 architecture performed significantly worse. Meaning different architectures synergize better with different types of systems. We can also see in Figure 5, that architectures perform differently compared to each other. In the case of systems with 16 satellites, the retrograde architecture slightly outperforms the cross-architecture, while using architectures compromised of 32 and 64 satellites, the clear winner is the cross-architecture.
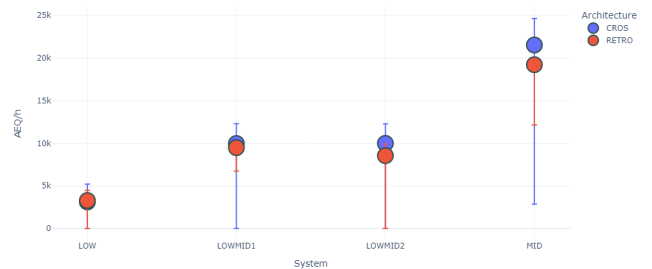

Fig. 5. The two main architectures side by side. The cross architecture-based systems are marked with blue, while the retrograde architecture-based systems are marked in red. The markers tag the average AEQ/h of the system, while the error bars visualize the minimum and maximum of said system.

In this paper, we demonstrated that by using non-continuous channels of communication it is possible to realize a quantum network over scarcely populated satellite systems.

The satellite systems presented here provide a great overview of the possible interactions between architectures and systems. Even though these interactions should be more deeply researched in their own paper.

REFERENCES

[1] Peter Shor. "Algorithms for Quantum Computation: Discrete Logarithms and Factoring". In: *Proceedings of 35th Annual Symposium on Foundations of Computer Science* (Oct. 1996). DOI: 10.1109/SFCS.1994.365700.

[2] Lov Grover. "From Schro¨dinger's equation to the quan- tum search algorithm". In: *Pramana-journal of Physics - PRAMANA-J PHYS 56* (Feb. 2001). DOI: 10.1007/s12043-001-0128-3.

[3] S. Imre. "Quantum Existence Testing and Its Ap- plication for Finding Extreme Values in Unsorted Databases". In: *IEEE Transactions on Computers 56* (2007). DOI: 10.1109/TC.2007.1032.

[4] Sara Gaily and Sándor Imre. "Quantum Optimization of Resource Distribution Management for Multi-Task, Multi-Subtasks". In: *Infocommunications Journal 11* (Jan. 2019), pp. 47–53. DOI: 10.36244/ICJ.2019.4.7.

[5] W. K. Wootters and W. H. Zurek. "A single quantum cannot be cloned". en. In: *Nature* 299.5886 (Oct. 1982), pp. 802–803. ISSN: 1476-4687. DOI: 10.1038/299802a0. URL: https://www.nature.com/articles/299802a0.

[6] Charles H. Bennett and Stephen J. Wiesner. "Communication via one- and two-particle operators on Einstein-Podolsky-Rosen states". In: *Phys. Rev. Lett.* 69 (20 1992), pp. 2881–2884. DOI: 10.1103/PhysRevLett.69.2881. URL: https://link.aps.org/doi/10.1103/PhysRevLett.69.2881.

[7] Matthäus Halder et al. "Entangling independent photons by time measurement". en. In: *Nature Physics 3.10* (Oct. 2007), pp. 692–695. ISSN: 1745-2473, 1745-2481. DOI: 10.1038/nphys700. URL: http://www.nature.com/articles/nphys700.

[8] I. S. Kabanov et al. "Practical cryptographic strategies in the post-quantum era". In: *Moscow, Russia, 2018*, p. 020021. DOI: 10.1063/1.5025459. URL: http://aip.scitation.org/doi/abs/10.1063/1.5025459.

[9] *Secure communication via quantum cryptography*. URL: https://www.esa.int/Applications/Connectivity_and_Secure_Communications/Secure_communication_via_quantum_cryptography.

[10] Sheng-Kai Liao et al. "Satellite-Relayed Intercontinental Quantum Network". In: *Phys. Rev. Lett. 120* (3 2018), p. 030501. DOI: 10.1103/PhysRevLett.120.030501. URL: https://link.aps.org/doi/10.1103/PhysRevLett.120.030501.

[11] *European Quantum Communication Infrastructure (EuroQCI) | Shaping Europe's digital future*. en. URL: https://digital-strategy.ec.europa.eu/en/policies/european-quantum-communication-infrastructure-euroqci (visited on 12/12/2021).

[12] Canadian Space Agency. Quantum Encryption and Science Satellite (QEYSSat). 2020. URL: https://www.asc-csa.gc.ca/eng/satellites/qeyssat.asp.

[13] Pengfei Wang et al. "Single ion qubit with estimated coherence time exceeding one hour". en. In: *Nature Communications 12.1* (Dec. 2021), p. 233. ISSN: 2041-1723. DOI: 10.1038/s41467-020-20330-w. URL: http://www.nature.com/articles/s41467-020-20330-w.

[14] Sumeet Khatri et al. "Spooky action at a global distance: analysis of space-based entanglement distribution for the quantum internet". en. In: *npj Quantum Information 7.1* (Dec. 2021), p. 4. ISSN: 2056-6387. DOI: 10.1038/s41534-020-00327-5. URL: http://www.nature.com/articles/s41534-020-00327-5.

[15] H.-J. Briegel et al. "Quantum Repeaters: The Role of Imperfect Local Operations in Quantum Communication". en. In: *Physical Review Letters 81.26* (Dec. 1998), pp. 5932–5935. ISSN: 0031-9007, 1079-7114. DOI: 10.1103/PhysRevLett.81.5932. URL: https://link.aps.org/doi/10.1103/PhysRevLett.81.5932.

[16] Donghai Huang et al. "Quantum Key Distribution Over Double-Layer Quantum Satellite Networks". In: *IEEE Access 8* (2020), pp. 16087–16098. ISSN: 2169-3536. DOI: 10.1109/ACCESS.2020.2966683. URL: https://ieeexplore.ieee.org/document/8959199/

[17] Yishu Wang et al. "Time-Dependent Graphs: Definitions, Applications, and Algorithms". en. In: *Data Science and Engineering 4.4* (Dec. 2019), pp. 352–366. ISSN: 2364-1185, 2364-1541. DOI: 10.1007/s41019-019-00105-0. URL: http://link.springer.com/10.1007/s41019-019-00105-0.

[18] Jian-Wei Pan et al. "Experimental Entanglement Swapping: Entangling Photons That Never Interacted". en. In: *Physical Review Letters 80.18* (May 1998), pp. 3891–3894. ISSN: 0031-9007, 1079-7114. DOI: 10.1103/PhysRevLett.80.3891. URL: https://link.aps.org/doi/10.1103/PhysRevLett.80.3891.

[19] Luc Maisonobe, Véronique Pommier, and Pascal Parraud. "Orekit: an open-source library for operational flight dynamics applications". In: *Proceedings of the 4th International Conference of Astrodynamics Tools and Techniques*. Apr. 2010.

[20] Quantum Satellite Communication Simulator. URL: https://www.mcl.hu/quantum-old/simulator/(visited on 10/03/2021).

[21] James F. Allen. "Maintaining knowledge about temporal intervals". en. In: *Communications of the ACM 26.11* (Nov. 1983), pp. 832–843. ISSN: 0001-0782, 1557-7317. DOI: 10.1145/182.358434. URL: https://dl.acm.org/doi/10.1145/182.358434.

[22] Zichang Zhang et al. "High-performance quantum entanglement generation via cascaded second-order non-linear processes". en. In: *npj Quantum Information 7.1* (Dec. 2021), p. 123. ISSN: 2056-6387. DOI: 10.1038/s41534-021-00462-7. URL: https://www.nature.com/articles/s41534-021-00462-7.

András Mihály graduated from Göllner Mária Regional Waldorf secondary school and earned his BSc degree in 2021. In 2020, he achieved 3rd place in the local Scientific Student Conference. He attended the 73rd International Astronautical Congress as a speaker. In 2022 he received 2nd place in the same Scientific Student Conference. He then completed his MSc in Computer Engineering at the Budapest University of Technology and Economics (BME) at the beginning of 2023. Currently, András is conducting research in the field of quantum computing.

László Bacsárdi (M'07) received his MSc degree in 2006 in Computer Engineering from the Budapest University of Technology and Economics (BME) and his PhD in 2012. He is a member of the International Academy of Astronautics (IAA). Between 2009 and 2020, he worked at the University of Sopron, Hungary in various positions including Head of Institute of Informatics and Economics. Since 2020, he is associate professor at the Department of Networked Systems and Services, BME and head of Mobile Communications and Quantum Technologies Laboratory. His current research interests are quantum computing, quantum communications and ICT solutions developed for Industry 4.0. He is the past chair of the Telecommunications Chapter of the Hungarian Scientific Association for Infocommunications (HTE), Vice President of the Hungarian Astronautical Society (MANT). Furthermore, he is member of AIAA, IEEE and HTE as well as alumni member of the UN established Space Generation Advisory Council (SGAC). In 2017, he won the IAF Young Space Leadership Award from the International Astronautical Federation.